

## Model for phonon transmission through a NbN grain-size distribution: Comparison with tunneling-spectroscopy observations

R. Chicault and Y. Joly

*Laboratoire de Spectrométrie Physique, Université Joseph Fourier (Grenoble I),  
Boîte Postale 87, 38402 Saint-Martin-d'Hères CEDEX, France*

(Received 17 April 1990; revised manuscript received 20 June 1990)

Transport properties of phonons in granular NbN thin film with  $\langle 111 \rangle$  texture are discussed. We propose a model in which each grain has an acoustic resonance when phonons propagate parallel to the film and where a coupling through the amorphous boundaries exists. A statistical study shows that the most homogeneous chains in the grain stack are selected because of the strong efficiency of their transport properties and that they give a fine structure of phonon modes even if the grain-size distribution is quite large. A reasonable agreement is obtained between our tunneling-spectroscopy experiments and the model. A typical experimental result has been fitted using an inelastic phonon-electron-interaction mean free path  $\Lambda_{\text{ph}} \approx 215$  nm and a mean grain size  $d_M \approx 25.7$  nm, the full width at half maximum of the grain distribution being 14 nm.

### I. INTRODUCTION

Electron transport properties in random-thickness pseudosuperlattices and/or in inhomogeneous media have been topics of many studies and are presently attracting further interest.<sup>1,2</sup>

For example, Kirtley *et al.*<sup>3</sup> recently observed a structure in the  $dI/dV$  curve of a granular niobium nitride (NbN) film obtained with a scanning tunneling microscope. They explained the general trends of the dynamic conductance of their sample by a charging effect, but did not comment on details of this structure. In their experiment, only a small number of grains in front of the tip of the microscope can play a role, and therefore electrons tunnel at an energy which depends on the grain size through its capacitance. Such structures were also observed by Ruggerio and Barner<sup>4</sup> in multilayer systems, where small metallic particles were enclosed between insulating artificial barriers. These structures were later interpreted by Barner *et al.*<sup>5</sup>

In contrast, very few studies concern transport properties of phonons in crystalline granular media. Apart from experimental problems, the main reason resides in the lack of a model to give a correct interpretation of the data. In a previous work, using tunneling spectroscopy on NbN-based Josephson junctions,<sup>6</sup> we observed sharp and complex structures at low energies (1–10 meV) in the  $dV/dI$  and  $d^2V/dI^2$  spectra. Such specific features were found with NbN-oxide-Pb(In) and NbN-oxide-NbN junctions. In both cases, the NbN base electrodes were identical, whereas in the latter case, the NbN counterelectrode was made of grains which were smaller than those of the base electrode. A transmission-electron-microscopy (TEM) analysis revealed that these base electrode films are made of columnar grains perpendicular to the oxide barrier. Moreover, in a plane parallel to the barrier, a distribution of grain sizes was observed. The

fine structures were explained by means of a pseudosuperlattice effect of phonons in the grains of the base electrode.

Our measurements were performed on  $3 \times 3 \mu\text{m}^2$  junctions. As a result, the number of grains concerned in the tunneling characteristic is very large ( $> 10^4$ ). In the case of charge effects, one should observe voltage steps having values in the range 1–4 meV, assuming that the relative dielectric permittivity of the insulating grain boundaries is 30 and that the area is the cross section of each grain which is in contact with the barrier. The presence of the aforementioned size distribution would then yield smooth bumps broader than 3 meV and not the fine structures which have been observed.<sup>6</sup> Thus another explanation for our spectrum has to be proposed.

In the present article, we propose a simple model intended to simulate the propagation of phonons across a pill of grains of inhomogeneous size. We show that, although a large size distribution  $p(d)$  is observed by TEM, narrow phonon modes can exist in the base electrode. We then show how these propagation modes are related to tunneling properties of an  $S_1$ - $I$ - $S_2$  Josephson junction (where  $S_1$  and/or  $S_2$  are the NbN granular films).

### II. MODEL

#### A. Introductory remarks

In the NbN system, we consider a phonon excited by a quasiparticle near the tunnel barrier. On average, the phonon will transfer its energy back to another electron after a distance  $\Lambda_{\text{ph}}$  equal to the inelastic electron-phonon-interaction mean free path. Therefore, one has to consider a statistical problem of phonon propagation, at an energy  $E$ , through grain chains of length  $\Lambda_{\text{ph}}$ .

As described earlier,<sup>6</sup> the NbN base electrode was

columnar with a strong  $\langle 111 \rangle$  texture perpendicular to the barrier, with typical grain heights in the range 50–100 nm. Each grain is separated from its neighbors by an amorphous region of width  $dt$ . Because of the hexagonal symmetry, there are six equivalent in-plane directions for phonon propagation parallel to the barrier.

Only those phonons whose wavelengths are of the order of the grain size are considered in our model, i.e., their wavelengths are equal to or greater than a few tens of the lattice constant. This has two consequences. First, at these low energies the phase velocities of the waves are energy independent. Second, the frequencies of elastic waves are proportional to the momentum. In other words, the energies of the modes are distributed in harmonics. Thus the problem can be treated with a classical approach, considering the acoustic modes inside the grains as the result of propagating elastic waves, which give, by partial reflection on the grain boundaries, pseudostationary or resonant waves.

For this reason, it is possible to use one of two different analogs: a mechanical analog or an electrical one. The mechanical analog consists of a chain of different vibrating springs and masses, weakly coupled to each other by their various spring constants, taking into account some friction to simulate the damping effects. We have chosen the second analog, which consists of coupled *LCR* circuits in which the presence of harmonics is allowed.

In order to simplify the model, we will consider, in the following, that the plane has isotropic properties with respect to phonon propagation. In addition, we assume that the grain shapes, in this plane, are approximately hexagonal. A phonon emitted from one grain propagates through other grains, keeping its coherence perpendicular to the way of propagation, just on the width of the crossed grains. Thus phonons cannot be considered as laterally infinite waves, and the problem therefore reduces from two dimensional (2D) to one dimensional (1D) along the path. A statistical approach then becomes sufficient to evaluate the probability of traversing each possible path.

Thus the phonon propagation can be described by the following steps: the transmission through a particular 1D chain made of a specific number of grains with specific sizes; the weighting by the probability of finding this particular chain where the probability depends on the number and on the size of the grains; the summation over all the types of chains of weighted admittance to get the efficiency  $\mathcal{E}(E)$  of the medium. This result is equivalent to a vibration mode density function of the energy. These three steps are developed in Secs. II B, II C, and II D.

One then has to find the relationship between these modes and the tunneling current of quasiparticles by means of electron-phonon coupling. This tunneling current through the barrier depends on the probability of the occurrence of a mechanism during which the incoming electron must transfer its energy to a phonon, which, after propagation, must transfer its energy to another electron. This fourth step, describing the electron-phonon coupling and its influence on the tunneling current, is developed phenomenologically in Sec. II E.

## B. Chain transmission model

### 1. Modeling of the grains

The system consists of chains containing many grains, each of which has particular properties. Each grain is considered as a resonator and is characterized by its fundamental resonance frequency  $f_0$  and its unloaded acoustic factor  $Q$ . An equivalent electrical system would be a system of coupled *LCR* circuits.

Initially,  $Q$  has to be determined by an empirical law. Let us assume that  $Q = \lambda / \Delta\lambda$ , where  $\lambda = v / f_0$  is the phonon wavelength, and  $\Delta\lambda$  is of the order of the width of the grain boundary,  $dt = 1$  to 2 nm.  $f_0$  is related to the acoustic speed  $v$  by  $f_0 = v / 2d$ , where  $d$  is the grain size. In this work we only consider the longitudinal mode. The velocity  $v = 17\,730$  m/s of the phonon in NbN is deduced from the Weber calculation<sup>7</sup> along the  $\langle 110 \rangle$  direction. For the fundamental resonance  $\lambda/2$ ,  $Q$  would then be proportional to the grain size  $d$ . In addition, several harmonics of the order of  $p$  can appear with their own  $Q$  factor. This leads to a decreasing law versus  $p$ , so that

$$Q(p, d) = \frac{Q_M d}{p d_M} . \quad (1)$$

Here  $Q_M$  is the unloaded acoustic factor for the fundamental of grains of mean size  $d_M$ .

On the other hand, we must also discuss the influence of the roughly hexagonal shape of the grains whose boundaries are defects for the propagating waves. The phonon is inelastically scattered at the lateral grain boundaries. This effect will be strong if the wavelength  $\lambda$  is of the order of magnitude of the hexagon size and weaker if  $\lambda$  is shorter. Thus the scattering is expected to be weaker for large  $p$  values. This is in disagreement with Eq. (1). In other words, there is no clear evidence for how one should treat the variations of  $Q$  and, in the following, we keep  $Q$  constant with the harmonic order  $p$ . However, this constant was varied over a rather wide range from 10 to 100.

### 2. Influence of the grain boundaries

Since the acoustic energy is propagated from one grain to another through the thin amorphous boundaries, one has to calculate its energy dependence. Ziman has considered the transfer of vibrations for the case of a thick amorphous medium located between two crystalline media.<sup>8</sup> This phenomenological approach consists of calculating how an original incoming plane wave loses its phase ( $\phi$ ) coherence during the propagation along the  $z$  axis inside the amorphous medium because of the relative acoustic speed fluctuation  $\delta s$ :  $\delta\phi / 2\pi = (dz / \lambda)(\delta s / s_0)$ . Ziman uses the speed fluctuation coherence length  $L_z$ , which is related to the correlation function of  $\delta s$ :  $\rho_{\delta s} = \exp[-(z / L_z)^2]$ . In the case of thin amorphous boundaries ( $Z_0 \ll L_z$ ), the mean square deviation of the phase fluctuation is given by

$$\overline{\delta\phi^2} = (4\pi^2 k / \lambda^2)(\overline{\delta s^2} / s_0^2) Z_0^2 , \quad (2)$$

where  $k$  is a constant in the range of 1–3. The energy radiated at the output is then shown to be proportional to  $\exp(-\pi\phi^2)$ ,<sup>8</sup> so that

$$\exp(-\pi\phi^2) = \exp\{(-4\pi^3/\lambda^2)Z_0^2[1+(\delta s^2/s_0^2)]\}. \quad (3)$$

For simplicity we assume that  $\delta s^2/s_0^2 \ll 1$ , so that Eq. (3) reduces to  $\exp[(-4\pi^3/\lambda^2)Z_0^2]$ . For the transmitted amplitudes, the coupling  $c$  between two adjacent grains can be expressed as

$$c(\omega) = \exp[(-\pi/2)(\omega Z_0/s_0)^2]. \quad (4)$$

A similar approach to this problem is used by Pendry<sup>9</sup> and Glauber<sup>10</sup> to consider the temperature effects in low-energy electron diffraction. Temperature effects are accounted for in the Debye-Waller approximation, where the scattering amplitudes are affected by an exponential decay factor:  $\exp[-\frac{1}{2}\langle\{(\mathbf{k}-\mathbf{k}')\cdot\Delta\mathbf{P}\}^2\rangle_T]$ , where  $\mathbf{k}$  and  $\mathbf{k}'$  are the incident and outgoing wave vectors, and where  $\Delta\mathbf{P}$  is the displacement of the atoms off their equilibrium position. The similarity with our phonons leads us to substitute  $\omega/s_0$  in the place of  $|\mathbf{k}-\mathbf{k}'|$ , and replace  $\Delta\mathbf{P}$  with the thickness of the amorphous boundaries, thus giving for the transmitted amplitude a similar expression:

$$c(\omega) = \exp[-\frac{1}{2}(\omega Z_0/s_0)^2]. \quad (5)$$

### 3. Modeling of the chain

As we have said above, the crystal and its grains can be described as a set of circuits, which are equivalent to the electrical scheme shown in Fig. 1. The energy transfer varies as  $f^2$  ( $f \equiv \omega/2\pi$ ) from one circuit to the next, because, at the resonant frequency in the  $i$ th grain, the load resistor seen from the  $(i-1)$ th grain is  $m^2\omega^2/r$  (giving a power ratio of  $m^2\omega^2/r^2$ ). It is not realistic to have such a transfer frequency (energy) dependence for phonons. The transfer must either be a constant or a decreasing function of frequency. In an earlier model, a constant coupling index,  $n_0 = m\omega/r$ , was used. In the following, the calculations have been performed using Eq. (5), i.e.,  $n_0 = c(\omega)$ , which is a slowly decreasing function of  $\omega$ .

Energy is injected into the first grain by an electron [excitation  $I(\omega)$  and input coupling  $M$ ] and transferred from the  $n_g$ th grain to a second electron (which has the same coupling  $M$  to the output load resistor  $R_s$ ).

If the input current  $I$  is  $\omega$  independent, the response of the chain is then given by the current  $I_s$  in the output load resistor  $R_s$ . In a more standard way, the transfer admittance  $A_i$  is defined by

$$A_i = I_s(\omega)/I(\omega),$$

which can be written as

$$A_i = -jM\omega i_{n_g}/(R_s I),$$

where  $i_{n_g}$  is the current in the  $n_g$ th circuit and  $j \equiv \sqrt{-1}$ . To calculate the ratio  $i_{n_g}/I$ , we have to write  $n_g$  linear equations for the circuits. If  $Z_1, Z_2, \dots, Z_{n_g}$  are the serial impedances of the circuits with currents  $i_1, i_2, \dots, i_{n_g}$ ,

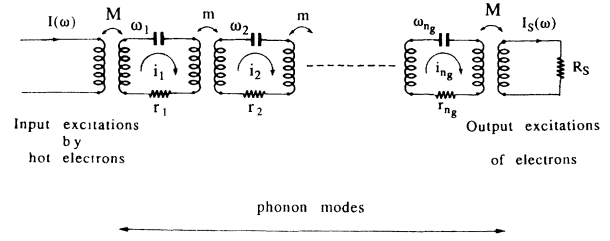


FIG. 1. Electrical representation of a grain stack with input and output coupling to the electron reservoir:  $I(\omega)$ , excitation current (excitation by quasiparticles supposed  $\omega$  independent);  $m$ , circuit coupling coefficient (transmission of energy by the grain boundaries);  $f_1, f_2, \dots, f_{n_g}$ , resonant frequencies of successive grains;  $M$ , input and output coupling coefficients (related to the electron-phonon coupling).

we can write

$$Z_1 i_1 + j m \omega i_2 = -j M \omega I,$$

$$Z_2 i_2 + j m \omega (i_1 + i_3) = 0,$$

...

$$Z_{n_g} i_{n_g} + j m \omega i_{n_g-1} + (M^2 \omega^2 / R_s) i_{n_g} = 0.$$

For convenience, the impedances  $Z_i$  can be written as  $Z_i = r(1 + jQ_0 v_i)$ , where  $v_i = \omega/\omega_i - \omega_i/\omega$ .  $\omega_i$  is a resonant self-angular-frequency in the  $i$ th circuit, and the current inside each grain  $i_i = p_i + j q_i$  is divided into real and imaginary parts. The system is then transformed into  $2n_g$  linear equations in real variables  $p$  and  $q$ .

In addition, for simplicity we divide each term by  $r$ , and set  $I = 1$ . Then, using the index  $n_0 = m\omega/r$  defined above, the system of  $n_g$  equations becomes

$$\begin{pmatrix} V_1 N_0 & \cdots & & & \\ N_0 V_2 N_0 & \cdots & & & \\ & \cdots & & & \\ \cdots & N_0 V_i N_0 & \cdots & & \\ & \cdots & & & \\ \cdots & N_0 V_{n_g} & & & \end{pmatrix} \begin{pmatrix} I_1 \\ I_2 \\ \vdots \\ I_i \\ \vdots \\ I_{n_g} \end{pmatrix} = \begin{pmatrix} S \\ 0 \\ \vdots \\ 0 \\ \vdots \\ 0 \end{pmatrix} \quad (6)$$

with the  $2 \times 2$  submatrices

$$V_i = \begin{pmatrix} 1 & -Q_0 v_i \\ Q_0 v_i & 1 \end{pmatrix} \quad \text{for } i = 1 \text{ to } n_g - 1,$$

$$V_{n_g} = \begin{pmatrix} 1 + M^2 \omega^2 / r R_s & -Q_0 v_{n_g} \\ Q_0 v_{n_g} & 1 + M^2 \omega^2 / r R_s \end{pmatrix},$$

$$N_0 = \begin{pmatrix} 0 & -n_0 \\ n_0 & 0 \end{pmatrix},$$

and the vectors

$$I_i = \begin{pmatrix} p_i \\ q_i \end{pmatrix} \quad \text{and} \quad S = \begin{pmatrix} 0 \\ -M\omega/r \end{pmatrix}.$$

We are then able to solve this system of equations for any angular frequency  $\omega$ . This allows us to calculate the transfer admittance  $A_i$  by introduction of the parameter  $Q_0$  and the index  $n_0$ , which is slightly smaller than 1 ( $n_0 = m\omega/r \lesssim 1$ ) if the coupling energy between two adjacent grains is strong enough.

#### 4. Influence of harmonics

An electric analog of each grain with its acoustical resonances is shown in Fig. 2. As we have seen above, when discussing the  $Q$  factor, the harmonic excitation involves some energy loss because of the diffusion of phonons and the friction of the atoms. This lost energy is proportional to the resistor values  $r_1, r_2, \dots, r_p, \dots$  (where 1 is the fundamental, and  $p$  the harmonic number). However, there is no evidence for a constant product  $rQ$  that allows one to relate  $r$  and  $Q$ , because the acoustic energy of successive modes does not fill exactly the same volume of grains.

The number of harmonics in any electrical or mechanical resonator is limited by the increasing losses versus the order. This increase depends on the nature of the system and is a complicated function of the harmonic order  $p$ . For example, if  $\lambda_1$  is the fundamental wavelength, for a plane wave  $e^{-jkx} = e^{-j(2\pi p/\lambda_1)x}$ , the damping is often described by a complex value of  $k$  leading to an  $e^{-p\alpha}$  term.

After a first attempt to perform numerical calculations to simulate the system with all the parameters  $r_p$  identical did not lead to satisfactory results (the envelope of the calculated structures diverges with increasing energy), all harmonics were allocated different  $r_p$  values. As a second step, we use a formula similar to that of a plane wave, where  $r_p = r_1 \exp[(p-1)/\gamma]$ , and  $\gamma$  is an adjustable parameter. However, the damping is still insufficient, and thus, in order to obtain a good envelope for the calculated structure when compared with experiment, we finally imposed the condition that

$$r_p = r_1 \exp \left[ \left( \frac{p-1}{\gamma} \right)^2 \right]. \quad (7)$$

The impedance  $Z$  can then be written as

$$Z = [(1/r_1)(1+jQ_1v_1) + (1/r_2)(1+jQ_2v_2) + \dots + (1/r_p)(1+jQ_pv_p) + \dots]^{-1}.$$

Simple transformations then allow us to write  $Z = Z_r + jZ_i$ , where the real and imaginary parts are separated. Moreover, for convenience, all values of  $r_p$  can be normalized to  $r_1$ , which is the resistance of the fundamental. Thus we use a normalized  $Z$  impedance given by

$$Z = [1/(1+jQ_1v_1) + (r_1/r_2)/(1+jQ_2v_2) + \dots + (r_1/r_p)/(1+jQ_pv_p) + \dots]^{-1},$$

which can also be written as  $Z = Z_{r1} + jZ_{i1}$ .

The matrix equation system (6) is now rewritten, re-

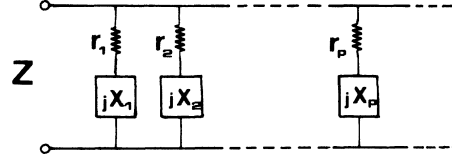


FIG. 2. Equivalent electrical circuit with harmonics inside the grains.

placing the real and the imaginary terms of each grain by  $Z_{r1}$  and  $Z_{i1}$ , respectively. The coupling between any two successive grains (defined in Sec. II B 3),  $n_0 = m\omega/r$ , is replaced by  $c(\omega)$  [Sec. II B 2, Eq. (5)] and the input-output coupling to the charge is given by  $\kappa = M\omega/R_s$ . Therefore, using  $R_s/r_1 = r_s$ , the matrix equation remains in the same form as in (6), but redefining,

$$\begin{aligned} V_i &= \begin{bmatrix} Z_{r1}(i) & -Z_{i1}(i) \\ Z_{i1}(i) & Z_{r1}(i) \end{bmatrix} \quad \text{for } i=1 \text{ to } n_g-1, \\ V_{n_g} &= \begin{bmatrix} Z_{r1}(n_g) + \kappa^2 r_s & -Z_{i1}(n_g) \\ Z_{i1}(n_g) & Z_{r1}(n_g) + \kappa^2 r_s \end{bmatrix}, \\ N_0 &= \begin{bmatrix} 0 & -c \\ c & 0 \end{bmatrix}, \end{aligned} \quad (8)$$

and

$$S = \begin{bmatrix} 0 \\ -\kappa r_s \end{bmatrix}.$$

### C. Statistical aspects of the model

#### 1. For each individual grain

The size distribution  $p(d)$  as observed by TEM in a similar NbN film is roughly in the range 20–31 nm for 50% of the grains, with a maximum in the probability at about  $d_M = 25$  nm (Fig. 3). For numerical calculations, a Gaussian distribution function of the variable  $(d_M/d - d/d_M)$  was used:

$$p(d) = \frac{1}{\sigma(2\pi)^{1/2}} \exp \left\{ -\frac{1}{2} \left[ \left( \frac{d_M}{d} - \frac{d}{d_M} \right) / \sigma \right]^2 \right\}. \quad (9)$$

In contrast to a Gaussian curve with  $|d - d_M|$  as the variable, the curve  $p(d)$  obtained using Eq. (9) is asymmetrical around  $d_M$  and is in better agreement with the curve that results from the TEM observations (see Fig. 3).

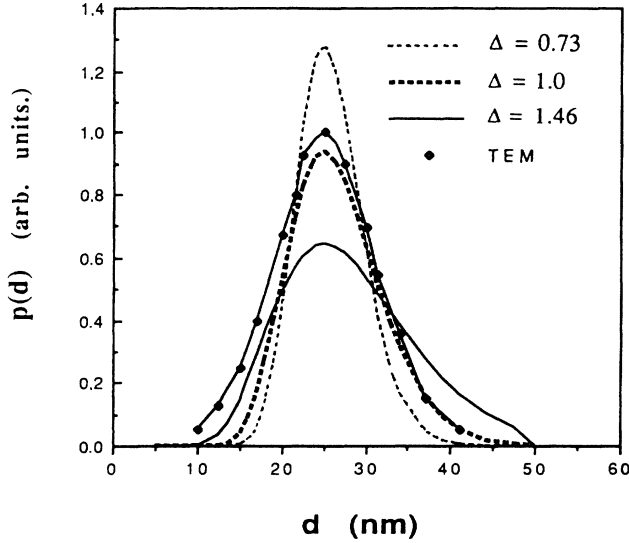


FIG. 3. Grain-size distribution from TEM observations ( $\diamond$ ), and a Gaussian fit of the variable  $(d_M/d - d/d_M)$ .

The adjustable parameters of the Gaussian (if the variable considered is  $d_M/d - d/d_M$ ) that we used are the full width at half maximum,  $\Delta = 2.355\sigma$ , and the most probable value of grain sizes  $d_M$ . For comparison, we give the curves  $p(d)$  for  $\Delta = 0.73, 1,$  and  $1.46$ .

## 2. For the two-dimensional structure of grain stack

If we consider a more realistic two-dimensional (2D) model, where phonons can propagate in the plane parallel to the barrier, many paths exist in any direction, and a few of them are selected due to their homogeneous grain width along the chains.

One can consider the hexagonal grain stack as a series

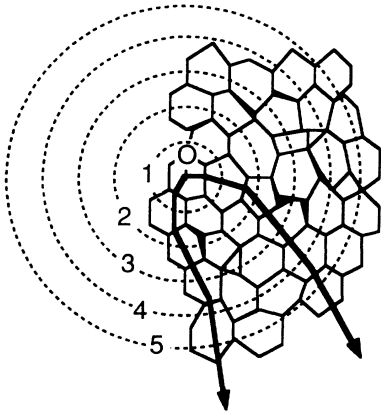


FIG. 4. Stack around any point and layered structure.

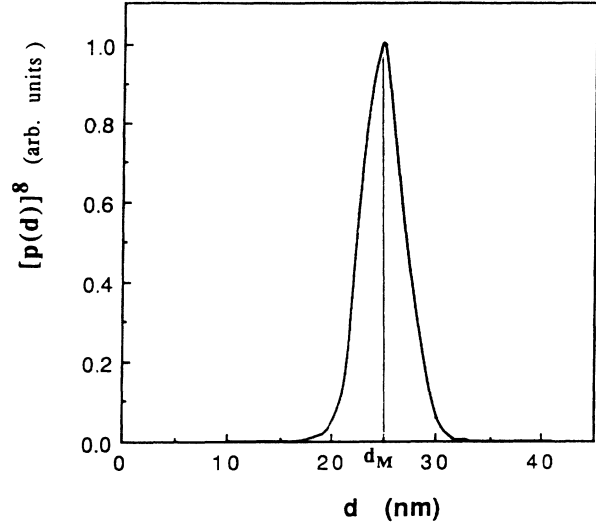


FIG. 5. Probability curve for eight grains, homogeneous in size (derived from the curve in Fig. 3).

of successive shells. We now look at the different possible ways for a phonon emitted from the grain in O (Fig. 4) to propagate through the shells. If the inelastic electron-phonon-interaction mean free path is  $\Lambda_{ph}$ , the phonon has to propagate through  $n_g = (\Lambda_{ph}/d_M) + 1$  grains (on average), a value that includes the central grain, before transferring its energy to an electron.

The total number of possible paths, through a collection of homogeneous grains of size  $d$ , is

$$\tau_d = \{p(d)\}^{n_g} \tau_T,$$

where  $\tau_T$  is the total number of possible paths. Thus the probability of propagation from a central grain of size  $d$ , through a homogeneous grain chain, is given by

$$\tau_d / \tau_T = \{p(d)\}^{n_g}.$$

The mean free path for an energy below the gap width,  $2\Delta_{NbN}$ , has been estimated to be around 300 nm,<sup>6</sup> and thus the number of grains crossed by the phonon is between 8 and 15. Even with a relatively large distribution  $p(d)$ , the probability  $\tau_d / \tau_T$ , with its power  $n_g$  between 8 and 15, becomes very sharp (Fig. 5). We are now able to understand that, even with an extended distribution curve, it is possible to observe fine structures in the transmission phonon spectra.

## 3. Calculation of probability in inhomogeneous chains

In reality, phonons can propagate through chains of grains which are not exactly homogeneous in size, but exhibit a dispersion which can be schematically characterized by the factor  $d_1/d_2$ ;  $d_1$  and  $d_2$  are, respectively, the size of the largest and the smallest grains in the chain under consideration.

The probability of obtaining such a chain is given by the following formula:

$$P(d_1/d_2, d_0) = \left[ \int_{d_2}^{d_1} p(d) dd' \right]^{n_g}. \quad (10)$$

This function depends on two parameters:  $d_1/d_2$ , and  $d_0 = (d_1 + d_2)/2$ , the average grain size in the chain.

At constant  $d_0$ ,  $P(d_1/d_2, d_0)$  increases monotonically versus  $d_1/d_2$  and converges asymptotically to the probability maximum for large  $d_1/d_2$ . As regards  $d_0$ ,  $P(d_1/d_2, d_0)$  becomes very small if  $d_0$  is much smaller or much larger than  $d_M$ . In our case, chains having  $d_0 < 19$  nm and  $d_0 > 36$  nm represent less than 1% of the possible paths.

#### 4. Calculation of transfer admittance versus dispersion

It is interesting to see how the transfer admittance  $A_t$  depends on the chain dispersion. The result shown in Fig. 6 gives the value of  $A_t$  at the energy (or frequency) corresponding to an average acoustic grains resonance of the chain under consideration, i.e.,  $f_0 = v/2d_0$ . The decrease of  $A_t$  is very strong with  $d_1/d_2$ , and this decrease becomes stronger when  $n_g$  increases because of a more efficient filter effect.

#### D. Acoustical efficiency of the system

Using the statistical probability given by Eq. (10) and the transfer admittance deduced in Sec. II B, one can obtain the real probability for the propagation of a phonon in a given system. We call this the efficiency  $\mathcal{E}(E)$ :

$$\mathcal{E}(E) = \int_{d_0} d(d_0) \int_{d_1/d_2} P(d_1/d_2, d_0) \times A_t(d_1/d_2, d_0, E) d(d_1/d_2). \quad (11)$$

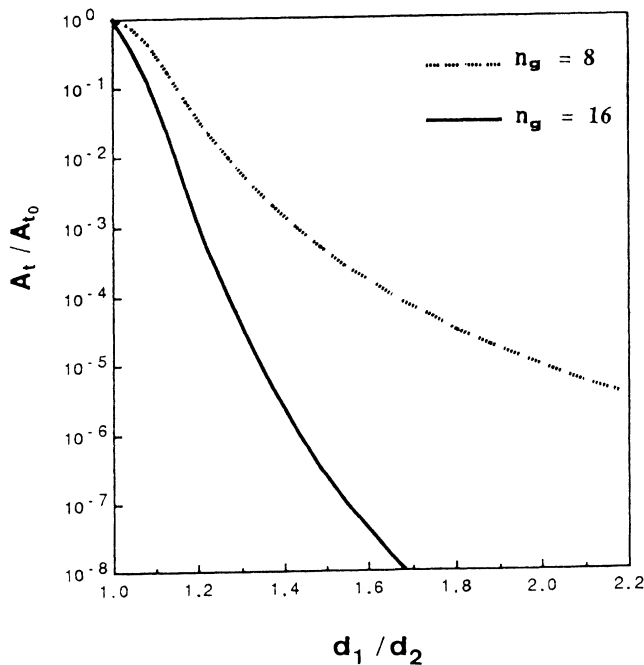


FIG. 6. Transfer admittance  $A_t/A_{t0}$  vs the dispersion ratio  $d_1/d_2$ , calculated for  $n_g=8$  and 16, and  $n_0=1$  ( $A_{t0}=5.95 \times 10^{-5}$  and  $1.71 \times 10^{-6}$  are the values of  $A_t$  for  $d_1/d_2=1$ ).

This quantity is proportional to an acoustical phonon-mode density, which depends on the energy  $E$ .

One has to sum over the dispersions  $d_1/d_2$  and the average sizes  $d_0$ . Since the transfer admittance  $A_t$  decreases rapidly with the frequency spreading ( $d_1/d_2$ ), while, in contrast, the weight function given by Eq. (10) increases (but has an upper bound), we expect that the efficiency will have a maximum. This is clearly shown in Figs. 7(a) and 7(b). The maximum value of the efficiency depends strongly on the width  $\Delta$  of the distribution  $p(d)$ , and as expected, the peak height increases for smaller values of  $\Delta$ . However, the maxima correspond to a value of  $d_1/d_2$ , which is approximately equal to 1.40.

The efficiency for  $n_g=8, 12$ , and 16 versus the variable  $d_1/d_2$ , given in Fig. 7(b), shows that the curves have the

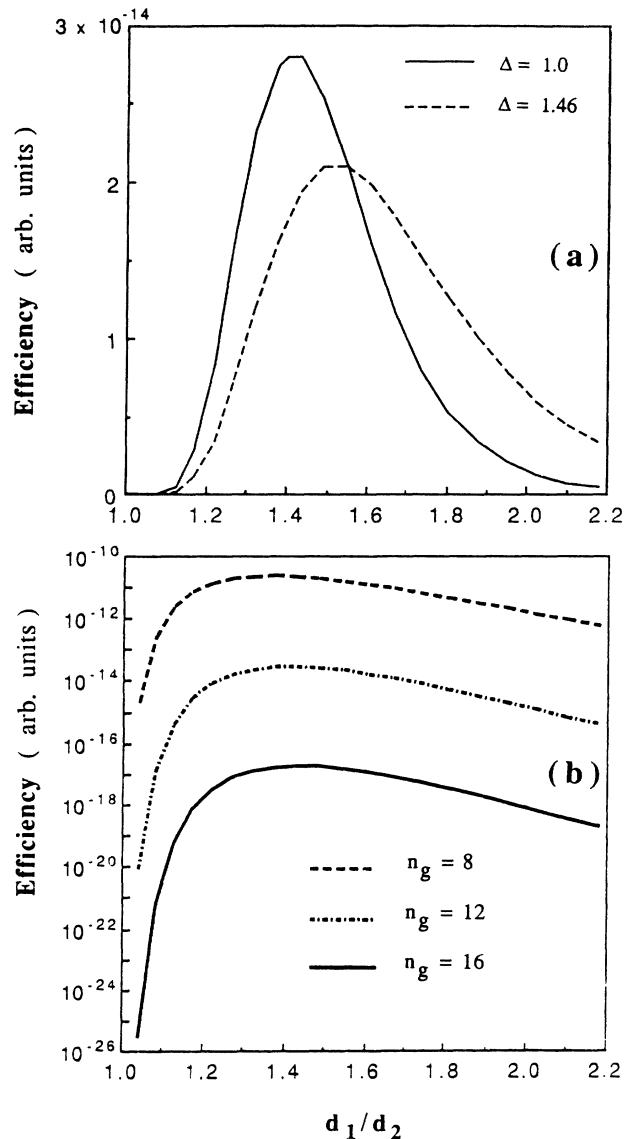


FIG. 7. Efficiency vs  $d_1/d_2$  calculated for  $n_g=12$ , with  $Q=20$  at the energy of fundamental,  $E=1.45$  meV, corresponding to  $d_M=25$  nm. (a)  $\Delta=1$ ;  $\Delta=1.46$  (values on y axis multiplied by 30). (b) Efficiency with the same parameters,  $\Delta=1$ , except that  $n_g=8, 12$ , and 16, showing evident maxima.

same shape with distinct maxima. The main difference is a factor of  $10^3$  and  $10^6$  in the efficiency for  $n_g = 8, 12,$  and  $16$ . From these preliminary results, it can be deduced that a good value for the efficiency will be reached only if the summations in Eq. (11) are expanded over large enough dispersions of chains. For instance, with  $\Delta = 1$  and  $d_1/d_2$  varying from 1 to 1.77, we just vary  $d_1/d_2$  in order to get  $P(d) \geq \frac{1}{2}[P(d)]_{\max}$ . The summation over a larger dispersion does not change the value of the efficiency.

### E. Relationship between electronic density of states and phonon-mode density

Having obtained the response of the grain system in terms of extra phonon modes, compared with acoustic modes of a monocrystal, which are particularly efficient above 10 meV, we now have to calculate the new low-energy electronic response in a tunneling experiment, where the electrodes are made of granular NbN. This can be done with use of the Eliashberg and Nambu theories. For convenience, we use a very simple empirical approach, which is exact enough, since we do not require an exact conductance  $dI/dV$  calculation, but only an estimate of the derivative  $d^2V/dI^2$  for comparison with experiments. By observing the results of MacMillan and Rowell<sup>11</sup> on lead and those of Bostock *et al.*,<sup>12</sup> and by making a comparison between the  $\alpha^2f(E)$  function (of the lead phonons) after exact deconvolution and the reduced density of states  $N_T(E)/N_{\text{BCS}}$ , it appears that  $N_T(E)$  is sufficiently well approximated by taking  $N_T(E)$  as

$$(E + \Delta_{\text{NbN}})/(E^2 + 2E\Delta_{\text{NbN}})^{1/2} + (K/E)d[\alpha^2f(E)]/dE$$

(zero energy is taken at gap edge). A coefficient  $K \ll 1$  (which is roughly adjusted) is added to the second term, so that the effect of phonon modes on  $N_T(E)$  should be around 1% compared with the BCS density of states; this number is not critical for our calculations. The conductance  $\sigma = dI/dV$  is then fitted using  $N_T(E)$ , and the second derivative  $d^2I/dV^2$  allows us to calculate  $d^2V/dI^2 = -\sigma^{-3}d^2I/dV^2$ .

## III. RESULTS

### A. Grain number fixed for all chains

At first, a series of calculations were performed with a grain number  $n_g$  fixed for all the chains. The results for grain boundaries  $dt = 1$  nm and  $\Delta = 0.73$  are given for  $n_g = 11$  and 17 [Figs. 8(a) and 8(b), respectively]. In each case, structures clearly appear at the fundamental (the energy associated with the mean grain size  $d_M$  by the formula in Sec. II B 1,  $f_M = v/2d_M$ ) and at the second harmonic together with broader peaks at 3.5 and 5–5.4 meV. These later peaks are related to the complicated combination of the weights and responses of each chain, but are not harmonics of  $f_M$ . When  $n_g$  increases, the structures seem to be narrowed but keep the general shape of the spectrum [only small differences appear between Figs. 8(a) and 8(b)]. In order to obtain envelopes of peaks which were comparable to the experiment, we modified

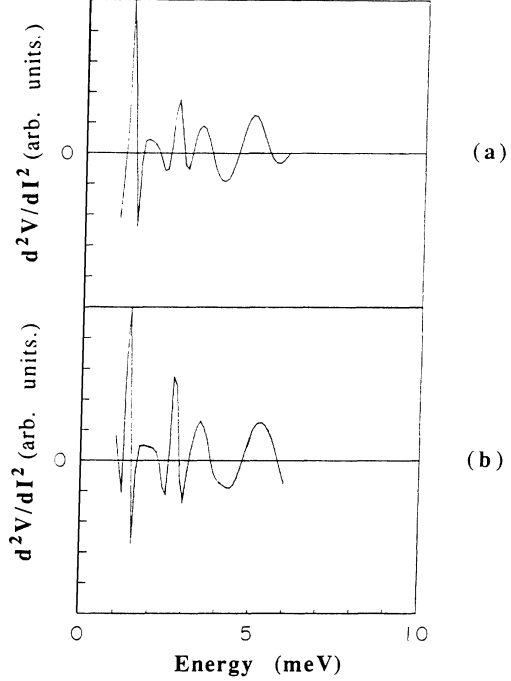


FIG. 8.  $d^2V(E)/dI^2$  calculated for  $\Delta = 0.73$ ,  $dt = 1$  nm. (a)  $n_g = 11$  and  $d_M = 26$  nm; (b)  $n_g = 17$  and  $d_M = 25$  nm.

$r_p$  and  $Q_p$ . Finally, we kept  $Q_p$  constant for all harmonics. Several calculations performed with a damping coefficient  $r_p = 1$  led to divergent peaks with increasing energy and were shown to be unrealistic.

### B. Phonon mean free path defines grain number

The calculation discussed above was a first approximation. In fact, for a given inelastic electron-phonon-interaction mean free path  $\Lambda_{\text{ph}}$ , phonons will propagate through a greater or lesser number of grains depending on their sizes.

We suppress the adjustable parameter  $n_g$ , which will now be taken as  $n_g = \Lambda_{\text{ph}}/d_0$ , where  $d_0$  is the average grain size in a chain.  $\Lambda_{\text{ph}}$  is the new adjustable parameter. When summing the response of each chain versus “average size,” one sums over chains which have lengths that are approximately fixed (in order to simplify the model), but with a different number of grains. The factor “number of grains” is a very important parameter for  $A_i$ , because it is at the boundary between two grains that the main part of the wave absorption occurs. This phenomenon is responsible for new fine structures (Fig. 9), which then result in the quantified variation (modulo 1) of the number of grains.

$\Lambda_{\text{ph}}$  is a very sensitive parameter, and it is possible to obtain a much improved agreement with the experimental curve. Figures 10(a) and 10(b) show spectra for  $\Lambda_{\text{ph}}$  equal to 300 and 375 nm. The number of sharp peaks increases with  $\Lambda_{\text{ph}}$ . In Fig. 11 the influence of the parameter  $\Delta$  (the width of the size distribution) is shown for the values  $\Delta = 1, 1.2,$  and  $1.3$ . As this parameter increases,

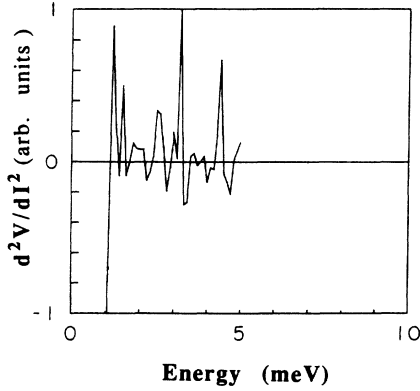


FIG. 9.  $d^2V(E)/dI^2$  calculated for  $\Lambda_{ph}=225$  nm,  $\Delta=1$ ,  $dt=1$  nm, and  $d_M=25.7$  nm.

the relative weight of the chains, with grains that are large (and small) compared to  $d_M$ , increases (see tails of the curve in Fig. 3). The response of low energies between 1 and 2 meV then increases strongly because many chains with a smaller number of grains exist. This is not surprising, because as  $\Delta$  increases, the number of groups of chains associated with a given value of  $d_0$  (or  $n_g$ ) also increases, and each group gives one structure at the fundamental  $f_0=v/2d_0$  ( $d_0 > d_M$  is the average value of grain size for chains contributing to the lower part of the curve). At higher energies, the already very squeezed structure is not and cannot be modified much.

Figure 12 shows the best fit between the (a) previously published experimental spectrum<sup>6</sup> and the (b) calculated

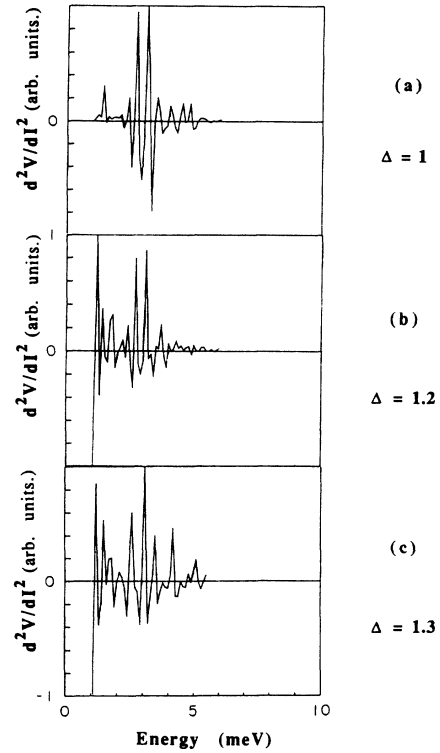


FIG. 11.  $d^2V(E)/dI^2$  calculated for  $\Lambda_{ph}=300$  nm,  $dt=1$  nm,  $d_M=25$  nm, and  $\gamma=4.2$ .  $\Delta$  is equal to (a) 1, (b) 1.2, and (c) 1.3.

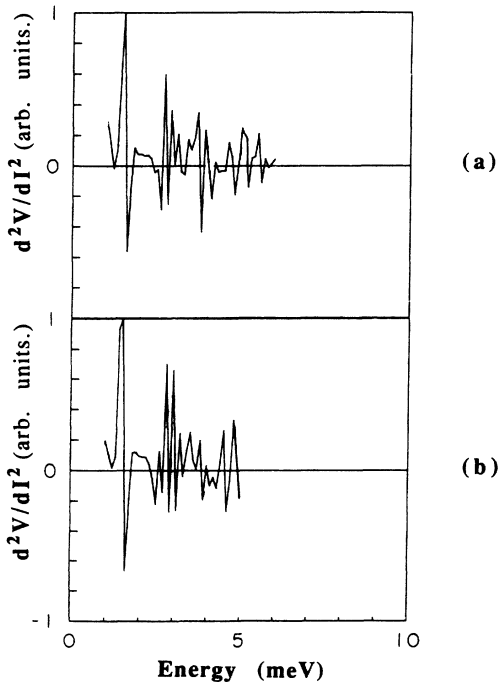


FIG. 10.  $d^2V(E)/dI^2$  calculated for  $\Delta=0.73$ ,  $dt=1$  nm,  $d_M=22.5$  nm, and  $\gamma=4.2$ .  $\Lambda_{ph}$  is equal to (a) 300 and (b) 375 nm.

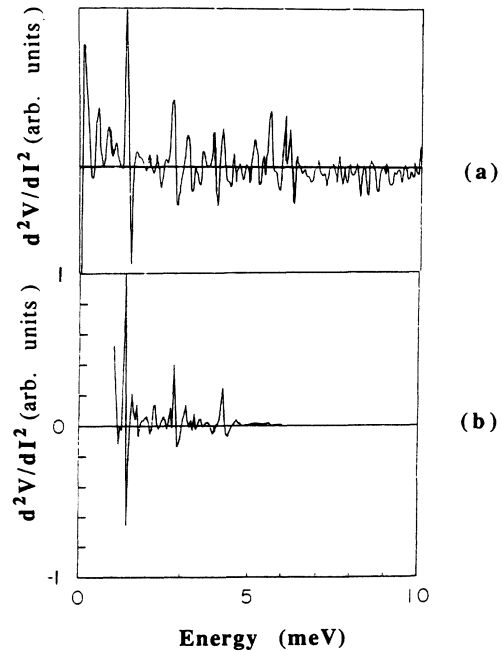


FIG. 12. (a)  $d^2V/dI^2$  experimental spectrum of Ref. 6 vs energy. (b)  $d^2V/dI^2$  calculated curve for  $\Lambda_{ph}=215$  nm,  $\Delta=1$ ,  $dt=1$  nm,  $d_M=25.7$  nm, and  $\gamma=3.2$ .

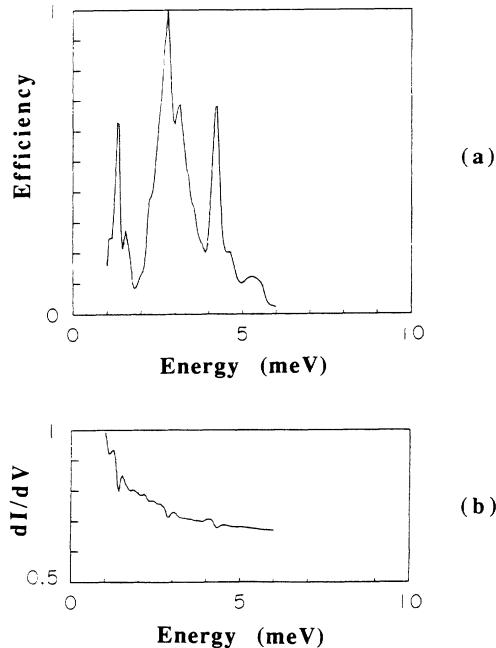


FIG. 13. (a) Efficiency vs energy, calculated with the same parameters as for Fig. 12. (b)  $dI(E)/dV$ , with the same parameters.

one. Values of the parameters are  $d_M = 25.7$  nm,  $\Delta = 1$  (which is equivalent to 14 nm),  $\gamma = 3.2$  in Eq. (7), and  $\Lambda_{ph} = 215$  nm. Since the result is very sensitive to  $\Lambda_{ph}$ , the uncertainty in  $\Lambda_{ph}$  is about 15 nm. Two other parameters of secondary importance were arbitrarily set, in order to satisfy  $\kappa^2 r_s < 1$  ( $\kappa = 0.175$  and  $r_s = 12.5$ ). Indeed, there is poor energy transfer from the last grain to the electron reservoir because of low values of electron-phonon coupling, even in the strong-coupling case. The predicted value of  $\Lambda_{ph}$  in a crystalline medium, given by the theory of Kaplan *et al.*,<sup>13</sup> at energies  $E < 6$  meV and for  $T/T_c < 0.2$ , is  $\Lambda_{ph} > 300$  nm. When a phonon reaches the junction edge (which measures approximately 1000 nm), it will be damped. This effect is not included in our calculation of the efficiency, and thus could partly account for the observed discrepancy.

Figures 13(a) and 13(b) show the efficiency, proportional to phonon-mode density, and also the approximated  $dI/dV$  curve.

Differences between the curves in Figs. 12(a) and 12(b) call for the following comments. We only include the longitudinal phonons in our model, but transverse acoustic modes can be excited and contribute to additional

structures. The grain model can probably be improved by a better knowledge of the relative  $Q_p$  and  $r_p$  parameters. The 5.5-meV peak of low amplitude in Fig. 13(a), which does not appear in Fig. 12(b), is probably a consequence of this. Finally, energy dependence of transmission through amorphous boundaries is only approximately known, and thus far all boundaries have been considered as being identical.

#### IV. CONCLUSIONS

We have presented a model that allows us to interpret the fine structures observed in a tunneling experiment, by means of collective intergrain vibration modes inside a medium made of grains with a large size distribution.

The main steps are the calculation of the decay of phonons propagating through grain chains, which are considered as coupled cavity filters, and a statistical treatment of all types of chains present in the medium, which leads to a phonon-mode density that is specific for the granular medium. In a phenomenological way, the electron-phonon interaction leads to the electron density of states and the derivative  $d^2V/dI^2$ .

The isotropic property of phonon transport is one of the keys of our model, and yields an acceptable agreement between experiment and theory.

This model can be applied to similar granular lattices or to artificial random superlattices, where phonons play a dominant role provided that the elementary cell (grain) can be sufficiently well described.

Although the best fit  $d^2V/dI^2$  exhibits minor differences with previous experimental results, our model is sufficiently close to the experimental curve to prove that, even with a fairly large grain size distribution, these collective modes act as resonators, and that their response is highly nonlinear, yielding narrow peaks.

The most important fitted parameters are the phonon mean free path  $\Delta_{ph} = 215 \pm 15$  nm, the mean grain size  $d_M = 25.7$  nm, and the full width at half maximum of the grain distribution (14 nm).

#### ACKNOWLEDGMENTS

The authors are indebted to Dr. Y. Gauthier for his fruitful collaboration, and Dr. R. Baudoing for helpful discussions. We would like to thank Dr. R. Rammal and Dr. M. Giroud for their suggestions, M. Schwerdtfeger and Dr. M. Lees for their careful reading of the manuscript. The Laboratoire de Spectrométrie Physique is "unité associée au Centre National de la Recherche Scientifique no. URA08."

<sup>1</sup>T. J. Godin and R. Haydock, Phys. Rev. B **38**, 5237 (1988).

<sup>2</sup>G. Wahlström and K. A. Chao, Phys. Rev. B **38**, 11 793 (1988).

<sup>3</sup>J. R. Kirtley, R. M. Fenestra, A. P. Fein, S. I. Raider, W. J. Gallagher, R. Sandstrom, T. Dinger, M. W. Shater, R. Koch, R. Laibowitz, and B. Bumble, J. Vac. Sci. Technol. A **6**, 259 (1988).

<sup>4</sup>S. T. Ruggiero and J. B. Barner, Phys. Rev. B **36**, 8870 (1987).

<sup>5</sup>J. B. Barner, K. Mullen, M. J. Honkanen, S. T. Ruggiero, E.

Ben-Jacob, and A. R. Pelton, in Proceedings of the Applied Superconductivity Conference, San Francisco, 1988 [IEEE Trans. Magn. **25**, 2542 (1989)].

<sup>6</sup>R. Chicaud and J. C. Villegier, Phys. Rev. B **36**, 5215 (1987).

<sup>7</sup>W. Weber, in *Superconducting in d- and f-Band Metals*, edited by H. Shul and M. B. Maple (Academic, New York, 1980), p. 131.

<sup>8</sup>J. M. Ziman, in *Electrons and Phonons*, edited by W. Marshall

- and D. H. Wilkinson (Oxford University Press, London, 1965).
- <sup>9</sup>J. B. Pendry, in *Low Energy Electron Diffraction*, edited by G. K. T. Conn and K. R. Coleman (Academic, London, 1974).
- <sup>10</sup>R. J. Glauber, *Phys. Rev.* **98**, 1692 (1955).
- <sup>11</sup>W. L. MacMillan and J. M. Rowell, in *Superconductivity*, edited by R. D. Parks (Dekker, New York, 1969).
- <sup>12</sup>J. Bostok, M. L. A. MacVicar, G. B. Arnold, J. Zasadzinski, and E. L. Wolf, in *Superconductivity in d- and f-Band Metals* (Ref. 7), p. 153.
- <sup>13</sup>S. B. Kaplan, C. C. Chi, D. N. Langenberg, J. J. Chang, S. Jafarey, and D. J. Scalapino, *Phys. Rev. B* **14**, 4854 (1976).